Recognition and Positioning of SBCs in BIM Models Using a Geometric vs Colour Consensus Approach

A. Adán, B. Quintana, S. A. Prieto

3D Visual Computing & Robotic Lab, University of Castilla La Mancha, Spain
E-mail: Antonio.Adan@uclm.es, Blanca.Quintana@uclm.es, Samuel.Prieto@uclm.es

Abstract –

This paper proposes a new approach that recognizes different kinds of small objects that are commonly seen on walls and ceilings of buildings (Figure 1). The general idea supported in this paper is that such objects, called service building components (SBCs), should be inserted into the structure of the standard existing as-is BIM models, as they are automatically generated. But identifying these small building components within the vast dataset provided by the scanner is a difficult issue not solved yet. Our approach first processes a dense coloured point cloud and extracts global geometry and colour features to identify potential SBCs. A novel consensus algorithm between geometry and colour features is the basis to efficiently recognize and calculate the position of the existing small objects in the as-is BIM model of the building. The method has been tested in real and simulated environments providing encouraging results.

Keywords –
Object recognition; Scan-to-BIM; Automatic BIM; 3D data processing.

1 Small building service components: the last semantic level of a BIM model

Many researchers are currently working on the automatic creation of as-is BIM models at several semantic levels. This paper is framed into the methods that automatically obtain some sort of 3D building model from 3D data. Nowadays, and roughly speaking, we can distinguish between four semantic levels which go from a mere point cloud model to a detailed 3D CAD model of the building structure.

The first semantic level covers the set of automatic data acquisition algorithms that provide a rough point cloud of the building. This model usually has a poor-semantic content and most of the research efforts are focused on finding an efficient scan planning algorithm, which provides a complete dataset of the indoors [1], [2] or outdoors [3] of buildings.

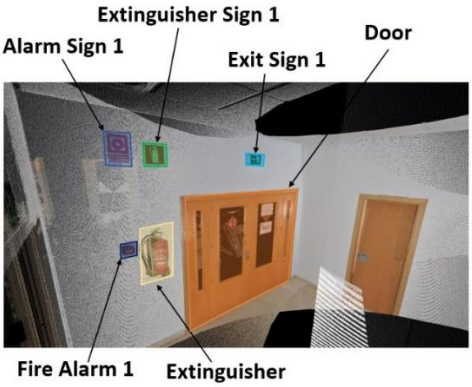

Figure 1. The image represents a coloured point cloud and different objects recognized in a wall. Apart from the doors, our recognition algorithm identifies five service building components.

The second level is achieved after processing the initial point cloud of the scene. The data are usually segmented into a set of representative parts, which follows specific geometric patterns (e. g. vertical/horizontal flat regions), and the scene is finally represented by a B-rep model. Essentially, this is a polyhedral model with certain attributes (i.e. vertex, edge and face) and their corresponding relationships. Works at this level can be found in [4], [5].

In the third level the segment extracted in the second level are recognized as essential constructive elements of the building. This is a higher semantic level in which a meaning of the earlier data segments is introduced. At this level, the model contains primarily objects such as “wall”, “ceiling”, “floor” and “column” ([6], [7]).

The fourth level completes the previous level by adding other important elements which lie in the constructive elements, such as windows, doors and frames. Examples of models at this level are that of references [8]–[10]. Other works include pipes or

scaffolding in the BIM models of industrial facilities ([11], [12]).

Beyond the fourth level, there are more components of a building that could be introduced in the BIM model as permanent or as-designed components. These small components are related with the habitability of the building, mainly related with power and security issues. As is argued in the abstract, from a constructive point of view, these components might have a relative importance, but are however essential for a safe and reliable life of the inhabitants of the building. Therefore, we propose a fifth level that includes such components which, from here on, we call service building components (SBCs). Previous work in the detection of SBCs is dealt in the next section.

2 Detection of SBCs: previous work.

Very few proposals achieve this level of detail in a 3D semantic building model and only partial solutions that recognise luminaries, sockets or other particular SBCs have been published to date. In addition, most of these works are framed in robot interaction applications.

Specific electrical equipment can be easily detected in thermal point clouds. For example, in [13] hot and cool regions are detected on ceilings. These regions are assumed to be electrical systems, heating, ventilation and air-conditioning components.

In [14], Díaz-Vilariño et al. process 2D coloured images of ceilings and identify two types of light fixtures. It is assumed that the segmented regions correspond to these objects, so that there is no proper recognition algorithm. Sockets and switches are also recognized in 2D images in [15]. Eruhimov et al. ([16]) classify between power holes, ground holes and the background in images acquired by a mobile robot. Meeussen et al. ([17]) recognize doors, door handles, electrical plugs and sockets, also under robotic applications.

Some authors provide more encouraging results. In [18], insulations, electrical outlets, studs and different states for drywall sheets are detected in 2D images. Unfortunately, the recognised objects are not positioned into a 3D model of the facility. The sensorial system presented by Bonanni et al. in [19] identifies - with the help of a human being- a set of usual small components, such as electrical outlets, fire extinguishers, hydrant boxes and printers. This is again a part of a human-robot system which is not related with the extraction of semantic models of buildings. The recognised small components are not therefore integrated into a 3D building model.

As is clear, the aforementioned SBCs detection methods are frequently associated with the recognition and pose estimation of objects in 2D images, which is not connected with an as-is semantically-rich 3D model of the building.

3 Justifying a new SBC recognition method in a BIM framework.

Recognition of SBCs in the BIM context is a difficult problem in which the origin and quality of the data to be processed plays an important role.

As is known, in general the problem of recognizing objects in 2D images has been extensively studied for many years and multitude of efficient solutions - including SIFT, SURF and others - have been proposed. All these algorithms commonly work on high quality images taken from medium/high resolution cameras, which signifies that the objects appear clear enough, with sufficient resolution and without significant superimposed noise. Nevertheless, object recognition in 2D images is restricted to merely identify, but not to estimate the position of the object in the 3D space (i.e. into a 3D indoor model).

Additionally, these techniques could yield frustrating results when applied to the raw scan data (the kind of data used for the construction of as-is 3D models), more precisely to the orthoimages generated from a coloured point cloud. Note that a balance between the resolution of the collected point cloud, the associated memory and the time requirements must be imposed in a building scanning process. On the other hand, in order to avoid occlusions, several scans must be taken (and later aligned) from different scanner positions. All this entails imprecisions on the coordinates of the registered data along with slight variations in the colour assigned to the surface of the potential SBCs (which have been viewed from different angles). Consequently, the orthoimages generated from the accumulated coloured point cloud are frequently, if not always, noisy and of a low resolution.

In practice, our automatic building scanning system generates orthoimages of 5mm/pixel. This resolution is achieved with an angular stepwidth of 0.065º, which yields 10 million points in 83 seconds per 360-scans. Of course, we can force the scanner up to a stepwidth of 0.0024º, but in this case, the system would become impractical.

To recognize a query (small) object in such a poor quality and low-resolution image (in fact, it is an orthoimage), new recognition methods need to be applied. The contributions of our approach lie in two pillars.

First, the geometry and colour data contained in the coloured point cloud are separately processed. Afterwards, the corresponding results are put in common by following an original consensus procedure. This is the most important issue of the paper, which is

explained in detail in Section 4.

The second pillar consists of avoiding local features and descriptors in the recognition algorithms. Since the orthoimages might appear blurred and with a poor colour quality, we define a supervised learning algorithm that uses a pattern composed of global descriptors, which are invariant to scale and rotation. In the experimental section, we briefly refer to a particular feature pattern that has provided encouraging recognition results.

Figure 2 illustrates the poor quality and low resolution of the SBCs' images contained in the orthoimage of the frontal wall of Figure 1. Note the poor quality of the fire-alarm switch image with 26x26 pixels in size (13x13 cm).

Figure 2. Images corresponding to BSCs in the scene shown in Figure 1.

4 A consensus framework for SBC recognition

4.1 Assumptions and inputs

The objective of this paper is not to explain specific recognition algorithms, but to propose a new approach that identifies and calculate the position of SBCs by means of a consensus between geometric and colour-based recognition strategies. We therefore present a consensus approach by assuming that a number of 3D processing stages have already been completed.

Let us consider that previous pre-processing stages, such as data collection, registration, colour fusion and initial data segmentation have successfully been carried out. Let us also assume that the accumulated point cloud has been segmented into the essential constructive elements of the building, including openings. According to the earlier semantic building model classification presented in Section 1, we start our SBC recognition approach on the basis that the fourth semantic level is available. At this level, the coloured point cloud associated with an already detected and modelled wall is therefore available. The reader can obtain complete information about our mobile mapping system for digitization (MoPAD) and our last works on extraction of automatic BIM models in references [20]–[22].

The set of coloured data belonging to a wall is structured as a 4D orthoimage, J_{CD}, in which each pixel has colour (RGB) and depth (i.e. an orthonormal distance between the 3D points and the wall plane). The colour and depth components of J_{CD} are decomposed into J_C (colour) and J_D (depth), and two different geometric and colour-based algorithms are afterwards applied on the respective orthoimages J_C and J_D.

Let us assume that, as a result of the earlier processes, for each expected object O_i, $i = 1 \dots N$, two lists of candidates $\{C\}_{O_i}$ and $\{D\}_{O_i}$are identified in both images J_C and J_D .

4.2 The Recognition Coherence Matrix

Since there could be more than one instance of the object O_i in the wall, after the consensus between the lists $\{C\}_{O_i}$ and $\{D\}_{O_i}$, the output could be composed of several regions (RoIs) located on the wall.

In order to evaluate all possible combinations of $\{C\}_{O_i}$ and $\{D\}_{O_i}$, we define a *Recognition Coherence Matrix* Ψ . Each entry in Ψ_{O_i} is the *Recognition Coherence Level* α, which measures the coherence between a pair of RoIs found in images J_C and J_D . This parameter is ranged in the interval [0,1] and will be defined below.

The flowchart in Figure 3 explains how Ψ is built for each query object, N being the number of SBC classes lying on the wall. Symbols n_C and n_D are formally: $n_C = \langle\{C\}_{O_i}\rangle$ and $n_D = \langle\{D\}_{O_i}\rangle$, where $\langle A\rangle$ represents the cardinal of the set *A*.

The *Recognition Coherence Level* α between two candidates is calculated by assessing the overlap between a pair of RoIs, B_C^j and B_D^k (with centroid coordinates c_C^j and c_D^k respectively) found in the respective images J_C and J_D . There are three cases:

1. Partial Intersection. B_C^j and B_D^k overlap. In this case, α measures the relative overlap with respect to the bounding box B_{CD}^{jk} that encloses B_C^j and B_D^k. The expression of α is given in equation (1).

$$\alpha = \frac{\langle B_C^j\rangle \cup \langle B_D^k\rangle}{\langle B_{CD}^{jk}\rangle} \tag{1}$$

2. No intersection. B_C^j and B_D^k does not overlap. In this case, $\alpha = 0$.
3. Exclusive detection. $\nexists B_C^j$ or $\nexists B_D^k$. In this case, O_i is only recognized in J_C or in J_D, and $\alpha = 0.5$.

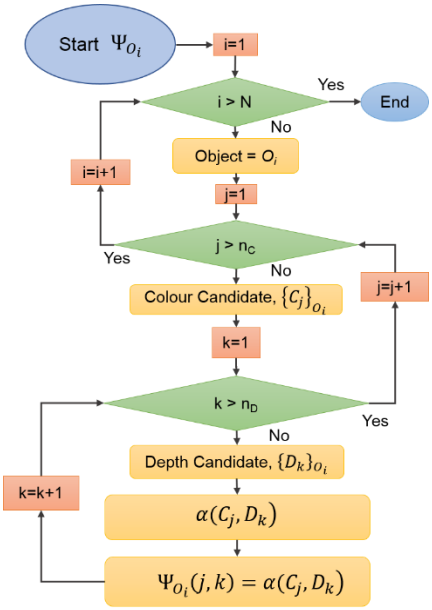

Figure 3. Algorithm for the construction of N *Recognition Coherence Matrices.*

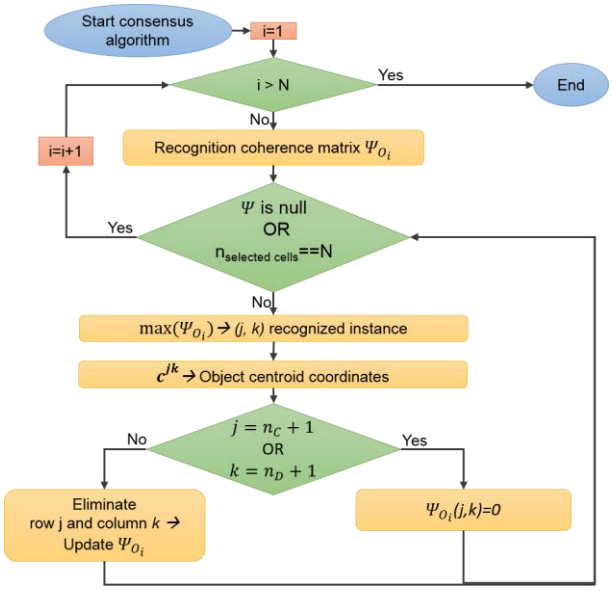

Figure 4. Recognition consensus algorithm.

4.3 Recognizing objects from the Recognition Coherence Matrix

The *Recognition Coherence Matrix* is completed with a new row and column, inserting the value 0.5 on them. The extra row and column are included because, besides the usual assignation of pairs of RoIs candidates, the exclusive detection by colour and depth is always considered in the resolution of the *Recognition Coherence Matrix*. In this way, Ψ_{O_i} is eventually a $(n_C + 1) \times (n_D + 1)$ matrix.

Once Ψ has been filled, the recognition consensus decision is solved iteratively following four steps (see Figure 4 for a better understanding):

4. The highest value of Ψ is selected and considered to be a recognized instance of the query object O_i.
5. The corresponding row and column of Ψ are eliminated, except when the selected cell corresponds to an exclusive detection case. In this case, only the corresponding cell is set to 0.
6. The coordinates of each recognized instance of the object O_i in the orthoimage J_{CD}, are calculated by means of a weighted mean of the corresponding RoIs centroid coordinates, $\boldsymbol{c_C^j}$ and $\boldsymbol{c_D^k}$.
7. Steps 1, 2 and 3 are iterated until Ψ is null or until the number of selected cells is equal to the number of expected instances of the query object in the wall.

Equation (2) shows two weights ρ_C^j and ρ_D^k that are defined depending on the specific geometric and colour based recognition algorithms used when the lists of candidates $\{C\}_{O_i}$ and $\{D\}_{O_i}$ are obtained. In our case, we take ρ_D^k as the cross-correlation coefficient, which is obtained when correlating the RoI B_D^k with that of the depth model of object O_i. The weight ρ_C^j is a normalized distance coefficient that evaluates the goodness of the recognition algorithm when comparing B_C^j with the colour model of object O_i. This is a minimum distance classifier algorithm that compares patterns composed of global colour features.

$$c^{jk} = \frac{\rho_C^j \boldsymbol{c_C^j} + \rho_D^k \boldsymbol{c_D^k}}{\rho_C^j + \rho_D^k} \tag{2}$$

4.4 Showing a case of study

In this section we explain in detail the recognition procedure in a representative case of study. We have simulated the digitization of an indoor floor using the Blensor software [23]. This tool allows us to simulate a scanning process on a 3D building model by using the same scanner we have got in our lab.

The indoor consists of several rooms with a wide set of SBCs lying on the walls. A representative wall of the room #4 has been taken to run our recognition strategy. This wall contains the following SBCs: an electric panel, two sockets, a switch, a fire extinguisher sign and an extinguisher (Figure 5 a)).

The orthoimage of the wall is decomposed into images J_C and J_D, and then processed separately. The

results obtained from the colour and depth-based algorithms yield two lists of candidates $\{C\}_{O_i}$ and $\{D\}_{O_i}$. Figure 5 b) highlights in blue the RoI candidates in images J_C and J_D. Note that the first columns show the colour model of the query objects.

Initially, some surprising candidates are assigned at this stage, particularly in the case of the colour-based recognition. For example, note that the region that contains the electric panel is within the list of candidates of the objects "socket" and "switch". The explanation of this apparently strange result is that we identify the regions in which the query object could be located and, since we use global colour descriptors, the recognition algorithm is invariant to the scale. Obviously, some of the global colour descriptors of the socket could match with that of the regions in which the electric panel lies, and for this very reason, this could be included in the list of candidates $\{C\}_{O_i}$.

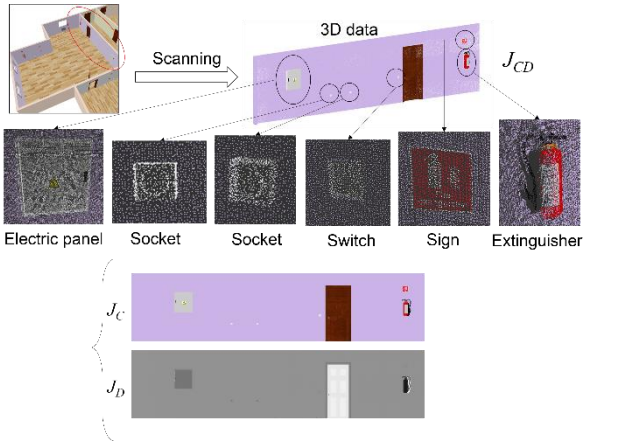

Figure 5. a) up) Representative wall of room #4 and the details of the coloured point clouds of the SBCs obtained from the virtual scanning. Down) Decomposition of the orthoimage J_{CD} into J_C (colour) and J_D (depth). b) The set of candidates $\{C\}_{O_i}$ and $\{D\}_{O_i}$ obtained after applying the recognition algorithms in images J_C and J_D. Candidate regions are highlighted in blue.

Since there are five different objects on the wall, five *Recognition Coherence Matrices* $\Psi_1, \Psi_2, \Psi_3, \Psi_4$ and Ψ_5 must be calculated. Figure 6 illustrates details of the Recognition Coherence Matrix Ψ_1 corresponding to the object "socket". Since $\langle\{C\}_{O_1}\rangle = 4$, $\langle\{D\}_{O_1}\rangle = 2$, Ψ_1 is a 5×3 matrix. The figure shows the positions of the candidates for each assigned pair and, according to the explained in Section 4.2, its corresponding overlapping type. Since we assume two instances of the object "socket" in the wall, the resolution process of Ψ_1 will take two iterations (See Figure 7).

As was explained in Section 4.3, the highest *Recognition Coherence Level* of Ψ_1 is taken as the first recognition result. This happens for the pair (C_3, D_2). The centre of the recognized instance of the object "socket" is then calculated according to equation (2). After deleting the corresponding row and column, the second assignation (C_2, D_1) is established and the same process follows. Since the number of selected cells is equal to the number of expected instances of the query object, the recognition process for the object "socket" comes to an end.

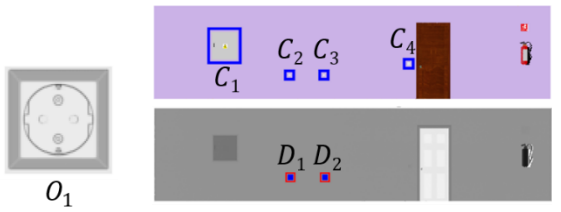

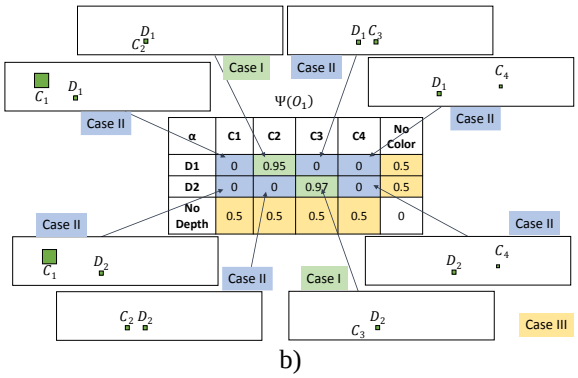

Figure 6. a) RoI candidates for the object "socket" in images J_C and J_D. b) The *Recognition Coherence Matrix* Ψ_1. Visualization of each pair of associated RoIs and the corresponding value of the *Recognition Coherence Level* in Ψ_1.

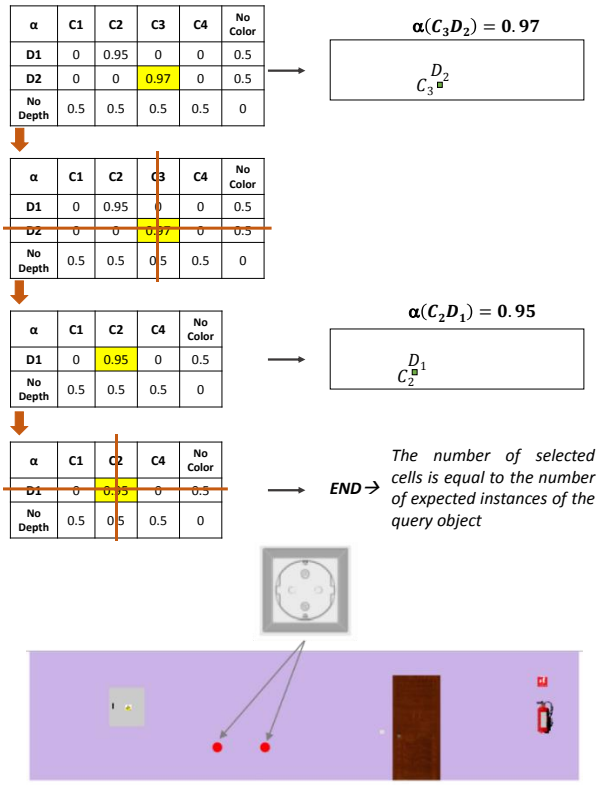

Figure 7. Solving the *Recognition Coherence Matrix* of the object "socket" and final recognition result.

5 Experimental test

This section is devoted to showing the efficiency of the geometric versus colour consensus approach in an experimental test. We simulated an indoor floor composed of 5 rooms containing 116 SBCs of 13 classes (See Figure 8). This scenario was virtually scanned with Blensor [23], which allows us to simulate the same real scanning process as with our Riegl VZ-400 3D laser scanner. In order to make the data acquisition process more realistic, noise to the position and colour of the collected point cloud was added.

The objective of this test is to compare the recognition results using, on one hand, separated colour-based and geometric-based algorithms (algorithm I and II in Table 1) and, on the other hand, the consensus approach (algorithm III in Table 1).

As mentioned in Section 4.3, our geometric-based recognition approach is a simple cross-correlation algorithm that compares the obtained RoIs B_D with that of the depth models of the objects existing on the wall. The colour-based recognition algorithm is a minimum distance classifier algorithm that takes some global colour features, such as the two principal saturation values in the HSV colour-space, the redness versus greenness and the yellowness versus blueness, which are parameters *a* and *b* in the Lab colour-space. Anyway, it is noteworthy to point out that the most important thing here is not in the specific geometric and colour-based algorithm applied, but in the efficiency of the consensus approach.

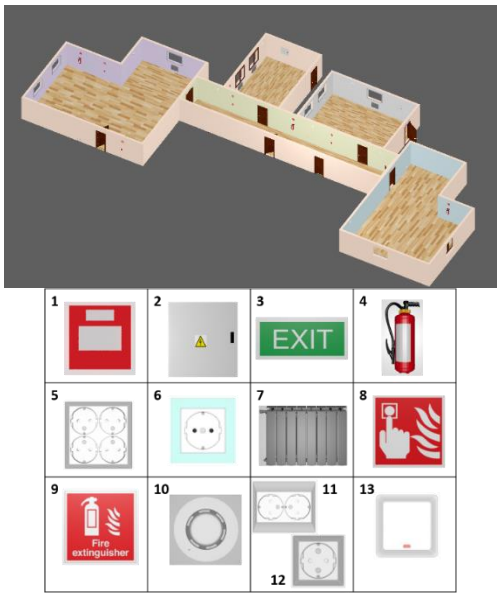

Figure 8. Simulated scenario used in the experimental test and the set of service building components included in the scenario.

Table 1. shows the recognition results after applying the aforementioned algorithms. The table includes the true positive cases (the algorithm recognizes successfully the query object), the false positive cases (the algorithm recognizes an object that is not the query object) and the false negative cases (the algorithm does not recognize the query object). Columns #1 to #5 refer to the five rooms of the scenario, column T is the total count and column Perc. signifies the recognition percentage.

The consensus algorithm achieves the greatest recognition percentages (90,5%) compared with algorithms I (83,6%) and II (41,4%). Although the geometric-based algorithm yields the lowest false positive percentage (5,2%), there is not a significant difference compared to that of the consensus algorithm (8,6%). In addition, the false positive rates are usually considered as the least important numbers in a recognition assessment. However, a more significant improvement can be seen in the figures concerning the false negative percentages. Clearly, the use of our consensus approach reduces the percentages yielded by the colour (16,4%) and the geometric-based (58,4%) approaches.

Figure 9 shows the extracted BIM model and the SBCs recognized after applying our algorithm. In this figure, each red spot represents the centroid of each recognized object.

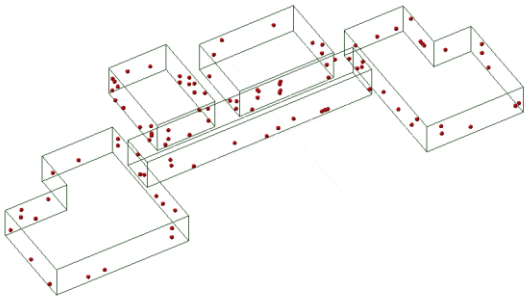

Figure 9. Recognition results superimposed onto the extracted as-is 3D model of the indoor floor. Red spots represent the recognized objects.

Table 2. provides more information about the false negative percentages for each one of the existing SBCs. In general, it can be stated that the objects with low-frequency colour/intensity components in the frequency domain (i. e. flat colour RoIs) are hardly detected by method I. Thus, the fire alarm switch (O_1), the electric panel (O_2) and the smoke detector (O_{10}) are not recognized in half of the cases. In regard to the method II, owing to the lack of depth discontinuity with respect to the wall, the regions with signs (e.g. O_8, O_9) and built-in sockets (e. g. O_6) are not detected as potential RoIs.

Note that the consensus algorithm decreases (or at least it is equal) the false negative percentages in all the cases. Significant improvements appear for the extinguisher (O_4), the socket x4 (O_5) and the smoke detector (O_{10}), in which both algorithms I and II fail. In O_4 and O_5, the false negative cases are eliminated and, in the case of O_{10}, the percentage in reduced up to 20%.

Table 1. SBC recognition results for the colour-based algorithm (I), the geometric-based algorithm (II) and the consensus approach (III). T=Total, Perc.=percentage

Algorithm		#1	#2	#3	#4	#5	T	Perc.
I	TP	20	24	18	21	14	97	83,6
	FP	4	1	5	5	1	16	13,8
	FN	4	3	5	5	2	19	16,4
II	TP	12	6	12	10	8	48	41,4
	FP	1	0	0	3	2	6	5,2
	FN	12	21	11	16	8	68	58,6
III	TP	23	25	21	22	14	105	90,5
	FP	1	1	2	4	2	10	8,6
	FN	1	2	2	4	2	11	9,5

Table 2. False negative percentages obtained per object.

Alg.	O_1	O_2	O_3	O_4	O_5	O_6	O_7
I	50,0	50,0	0	11,1	27,3	16,7	0
II	75,0	25,0	10,00	55,6	36,4	100	83,3
III	37,5	25,0	0	0	0	16,7	0
Alg.	O_8	O_9	O_{10}	O_{11}	O_{12}	O_{13}	Total
I	25,0	11,1	50,0	0	0	0	16,4
II	100	100	30,0	0	70,0	25,0	58,6
III	25,0	11,1	20,0	0	0	0	9,5

6 Conclusions

As is known, electric components (e. g. sockets and switches), fire devices (e. g. fire alarms and extinguishers) and a diversity of signs (e. g. exit signs and prohibition signs) are frequently placed inside the buildings, constituting a further but necessary part of the building. These small components, mostly related with the habitability of the building, should be included in the current as-is BIM models of buildings.

In order to recognize and estimate the position of such secondary components, this paper proposes a methodology that takes advantage of the geometric and colour information provided by the current 3D sensors (usually 3D laser scanners). But, owing to the poor quality and resolution of the orthoimages generated from the collected coloured point cloud, the SBC detection and its subsequent integration into the as-is 3D model of the building becomes a difficult problem, which needs to be addressed from new strategies.

The solution presented in this paper separates colour and geometric characteristics and proposes a consensus between the respective separated recognition results. This consensus has been implemented by means of the original concepts *Recognition Coherence Matrix* and the *Recognition Coherence Level*, which allows us to recognize multiple instances of the same object.

The method has successfully been tested on real and simulated data. The results yielded from the experimental work show that SBC recognition rates are greatly improved when our strategy is applied. These improvements signify that the use of the proposed consensus method makes the whole recognition process more robust and effective. In conclusion, our approach recognizes more objects and commits fewer identification failures, thus providing a rich fifth-level semantic 3D model of the building.

7 Acknowledgments

This work has been supported by the Spanish E.C. Ministry [DPI2016-76380-R project] and by the PREDUCLM16/23 UCLM human resource grant.

References

[1] Surmann H., Nüchter A. and Hertzberg J. An autonomous mobile robot with a 3D laser range finder for 3D exploration and digitalization of indoor environments. *Rob. Auton. Syst.*, 45(3–4): 181–198, 2003.

[2] Strand M. and Dillrnann R. Using an attributed 2D-grid for next-best-view planning on 3D environment data for an autonomous robot. *Proc. IEEE Int. Conf. Inf. Autom.*, 2008.

[3] Blaer P. S. and Allen P. K. Data acquisition and view planning for 3-D modeling tasks. *Int. Conf. Intell. Robot. Syst.*, pages 417–422, 2007.

[4] Jung J. *et al.* Productive modeling for development of as-built BIM of existing indoor structures. *Autom. Constr.*, 42:68–77, 2014.

[5] Wang C., Cho Y. K. and Kim C. Automatic BIM component extraction from point clouds of existing buildings for sustainability applications. *Autom. Constr.*, 56:1–13, 2015.

[6] Ochmann S., Vock R., Wessel R. and Klein R. Automatic reconstruction of parametric building models from indoor point clouds. *Comput. Graph.*, 54:94–103, 2016.

[7] Previtali M., Barazzetti L., Brumana R. and Scaioni M. Towards automatic indoor reconstruction of cluttered building rooms from point clouds. *ISPRS Ann. Photogramm. Remote Sens. Spat. Inf. Sci.*, 2014.

[8] Xiong X., Adan A., Akinci B. and Huber D. Automatic creation of semantically rich 3D building models from laser scanner data. *Autom. Constr.*, 31:325–337, 2013.

[9] Budroni A. and Boehm J. Automated 3D Reconstruction of Interiors from Point Clouds. *Int. J. Archit. Comput.*, 8(1):55–74, 2010.

[10] Valero E., Adan A., Huber D. and Cerrada C. Detection, Modeling, and Classification of Moldings for Automated Reverse Engineering of Buildings from 3D Data. *International Symposium on Automation and Robotics in Construction (ISARC)*, 2011.

[11] Czerniawski T., Nahangi M., Haas C. and Walbridge S. Pipe spool recognition in cluttered point clouds using a curvature-based shape descriptor. *Autom. Constr.*, 71:346–358, 2016.

[12] Turkan Y., Bosché F., Haas C. T. and Haas R. Tracking of secondary and temporary objects in structural concrete work - ProQuest. *Constr. Innov.*, 14(2):145–167, 2014.

[13] Kim P., Chen J., Cho Y. K., Kim P., Chen J. and Kwon Y. Building element recognition with thermal- mapped point clouds. *34th International Symposium on Automation and Robotics in Construction (ISARC 2017)*, 2017.

[14] Díaz-Vilariño L., González-Jorge H., Martínez-Sánchez J. and Lorenzo H. Automatic LiDAR-based lighting inventory in buildings. *Meas. J. Int. Meas. Confed.*, 73:544–550, 2015.

[15] Krispel U., Evers H. L., Tamke M.,. Viehauser R and Fellner D. W. Automatic texture and orthophoto generation from registered panoramic views. *Int. Arch. Photogramm. Remote Sens. Spat. Inf. Sci. - ISPRS Arch.*, 40(5W4):131–137, 2015.

[16] Eruhimov V. and Meeussen W. Outlet detection and pose estimation for robot continuous operation. *IEEE Int. Conf. Intell. Robot. Syst.*, pages 2941–2946, 2011.

[17] Meeussen W. *et al.* Autonomous door opening and plugging in with a personal robot. *Proc. - IEEE Int. Conf. Robot. Autom.*, pages 729–736, 2010.

[18] Hamledari H., McCabe B. and Davari S. Automated computer vision-based detection of components of under-construction indoor partitions. *Autom. Constr.*, 74:78–94, 2017.

[19] Bonanni T. M., Pennisi A., Bloisi D., Iocchi L. and Nardi D. Human-Robot Collaboration for Semantic Labeling of the Environment. *Proceedings of the 3rd Workshop on Semantic Perception, Mapping and Exploration*, 2013.

[20] Prieto S. A., Quintana B., Adán A. and Vázquez A. S. As-is building-structure reconstruction from a probabilistic next best scan approach. *Rob. Auton. Syst.*, 94:186–207, 2017.

[21] Quintana B., Prieto S. A., Adán A. and Vázquez A. S. Semantic Scan Planning for Indoor Structural Elements of Buildings. *Adv. Eng. Informatics*, 30(4): 643-659, 2016.

[22] Quintana B., Prieto S. A., Adan A. and Bosche F. N. Door Detection in 3D Coloured Point Clouds of Indoor Environments. *Autom. Constr.*, 85: 146-166, 2018.

[23] Gschwandtner M., Kwitt R., Uhl A. and Pree W. BlenSor: Blender sensor simulation toolbox. *Lect. Notes Comput. Sci. (including Subser. Lect. Notes Artif. Intell. Lect. Notes Bioinformatics)*, 6939(PART 2):199–208, 2011.